Available online www.jocpr.com

Journal of Chemical and Pharmaceutical Research, 2015, 7(4):1018-1023

Research Article

ISSN : 0975-7384
CODEN(USA) : JCPRC5

Effect of number of coatings on structure, mechanical properties and corrosion behaviour of HA coating on 316L stainless steel

Deepak Narang and Uma Batra

Department of Materials and Metallurgical Engineering, PEC University of Technology, Chandigarh, India

---

ABSTRACT

In this study, hydroxyapatite coatings were deposited on AISI 316L stainless steel using sol–gel dip coating method. The three coatings were developed by subjecting the substrate to three; four and five times dip in the sol. The surface morphology and elemental analysis of coatings were studied using scanning electron microscopy (SEM) and energy dispersive X-ray (EDX) spectroscopy. The porosity in coating was determined using inverted metallurgical optical microscope (Zeiss Axiovert 200 MAT) fitted with imaging software (Dexel, version 1.3.4). The surface roughness was determined using surface testing machine (Surftest, Mitutoyo, model SJ-400) for a cut-off of 0.8 mm. The micro hardness test on coated samples was conducted using a Vicker's micro hardness tester (model HV-1000 V, Huayin). The adhesion strength of the coatings was calculated using Hertz equation. The coating developed by four times dip demonstrated the minimum surface roughness; maximum micro hardness and adhesion strength. In order to investigate the corrosion behavior of uncoated and hydroxyapatite coated 316L stainless steel, electrochemical potentiodynamic polarization tests were performed in physiological solutions at 37±1°C. The coating developed by exposing substrate for four times dip in sol. offered a better corrosion protection of the substrate compared to coatings developed by exposing for three or five times dip in sol.

Keywords: 316L stainless steel, dip coating, hydroxyapatite, sol-gel, surface roughness, linear polarization

---

INTRODUCTION

Metals, polymers, ceramics and composites are being immensely employed to replace bones in surgery of the damaged parts. Among various materials available in the market, metallic biomaterials like titanium alloys and stainless steels are widely used for the implant surgery applications due to their good corrosion resistance and mechanical properties. There are many reports on improvement by employing hydroxyapatite (HA) coatings on the surface of the metallic implants [1-4]. Hydroxyapatite ($Ca_{10}(PO_4)_6(OH)_2$) is one of the most prominent biocompatible ceramic materials which promotes osseointegeration of implant materials to surrounding tissue due to its similar composition and structure to the human body [5-8]. A survey of literature reveals that there are many techniques employed for synthesis of HA coatings on the surface of metallic biomaterials. These include plasma spraying [9-11], sputtering [12,13], electrophoretic deposition [14-17] and sol-gel [19-24]. Among all the above methods sol-gel technique plays a vital role due to many advantages such as: (a) synthesis of thin or thick film with a high porosity area which improves the efficiency of sensor (b) modification in composition with uniformly dispersed dopants (c) easy control on film thickness (d) excellent homogeneity (e) ability to coat large area and complex shape (f) equipment's can be assembled at low cost (g) low temperature in processing. Generally there are three methods that are used in the sol-gel technique. These are spin coating, dip coating and spray coating. In this

study, dip coating method is applied to generate hydroxyapatite coatings on 316L SS. The effect of the number of coatings on structure and resistance to corrosion was analyzed.

EXPERIMENTAL SECTION

2.1Sample Preparation and sol gel dip coating

316L SS was used as a metal substrate with elemental composition given in Table 1. Type 316L SS alloy was cut into 15 mm x10 mm x 2 mm pieces. The 316L SS samples were polished using silicon carbide papers of 120, 220, 320, 400 and 600 grit. Final polishing was done using coarse (1μm) diamond paste in order to produce scratch-free mirror-finish surface. The polished specimens were degreased with acetone and thoroughly washed with distilled water. This was followed by ultrasonic cleaning in acetone for 10min.Then the samples were rinsed in deionised water and dried before application of coatings.

Table 1: Composition of 316L SS (wt. %)

Element	Cr	Ni	Mo	Mn	C	P	S	Si	V	Cu	Fe
wt. %	16.36	10.59	2.06	0.872	0.03	0.019	0.0003	0.60	0.047	0.091	Bal.

The HA coating on 316L SS substrates was synthesized by sol-gel method 0.1M calcium nitrate tetrahydrate, CNT (Merck, 99.9% Pure) and 0.3M phosphorus pentoxide, P_2O_5 (Merck, Pure) were prepared separately in 100ml ethanol (Merck, 99.9% pure). The CNT solution was added drop wise into the P_2O_5 solution to obtain Ca/P ratio of 1.67. The prepared 316L SS samples were dipped into this sol solution at a speed of 10mm/min. After dipping once the sample was withdrawn with the same speed as used for dipping to get uniform thickness. Now the coated substrate was dried by immediately transferring into an oven at 70°C for 10 minutes. This procedure was repeated for a number of times (1st substrate three times, 2nd substrate four times and 3rd substrate five times). The HA coated 316L SS samples were designated as HA-316L SS-3,HA-316L SS-4 and HA-316L SS-5, where the last digit indicates the number of times this procedure was repeated. The heat treatment was carried out on each substrate at 800°C for 1 hour in a muffle furnace.

2.2 Structural characterization

The coating surfaces were investigated using scanning electron microscope (JSM-6610LV with oxford attachment of EDX). The porosity in coating was determined by using inverted metallurgical optical microscope (Zeiss Axiovert 200 MAT) fitted with imaging software (Dexel, version 1.3.4). The porosity was determined at twenty separate locations and the average value is reported. The surface roughness was determined with a using surface testing machine (Surftest, Mitutoyo, model SJ-400) for a cut-off of 0.8 mm. An average five measurements carried out at different locations was taken. The micro hardness test on coated samples was conducted using a Vicker's micro hardness tester (model HV-1000 V, Huayin) with a load of 25gm and a dwelling time of 12 seconds. The adhesion strength of the coatings was calculated from the Vicker's micro hardness values by using Hertz equation:

$$\text{AdhesionStrength} = \left(\frac{\text{VHN}}{3}\right) 0.1^{\text{n}} \qquad \text{(Eq. 1)}$$

Where, VHN is the Vicker's Hardness Number, n is zero for ceramics.

2.3Potentiodynamic polarization test

The electrochemical corrosion behavior testing of HA coated 316L SS was performed in simulated body fluid (SBF) proposed by Kuboko and his co-workers [25] using a PGSTAT 12, Metrohm Autolab, the Netherlands with analysis software (ANOVA). A three-electrode cell was used with the sample as the working electrode, graphite and Ag-AgCl as the counter electrode and reference electrode, respectively. In order to simulate the conditions of the human body, the SBF solution was maintained at a temperature of 37 ± 1°C and at pH of 7.4. The 1cm^2 area of uncoated 316L SS, HA-316L SS-3, HA-316L SS-4 and HA-316L SS-5 sample was exposed to the electrolyte. After 3 hours of immersion in SBF, potentiodynamic polarization curves were obtained at a scan rate of 0.001 Vs^{-1} from -0.1 V vs. versus the open-circuit potential (OCP) to the breakdown of passive region. The corrosion current densities and corrosion potentials of various specimens were determined from these curves by Tafel extrapolation methods. The mean value and standard deviation of the results were also calculated. The linear Tafel segments to the anodic and cathodic curves (-0.1 to + 0.1 V versus corrosion potential) were extra polated to corrosion potential to obtain the corrosion current densities. The slope gives the Tafel slopes ($b_a$and b_c) and the intercept corresponds to corrosion current density i_{corr}. The i_{corr} (A/cm^2) was calculated using the Stern-Geary equation [26];

$$i_{corr} = \frac{b_a . b_c}{2.3(R_P)(b_a + b_c)} \quad \text{(Eq.2)}$$

Corrosion rate (*C.R*) in mm/year was calculated by using following relationship [27] equation 3;

$$C.R = 3.268 \times 10^3 \frac{i_{corr}}{\rho} \frac{MW}{z} \quad \text{(Eq. 3)}$$

Where *MW* is the molecular weight of the specimen (g/mole), ρ is density of the specimen (g/m^3) and *z* is the number of electrons transferred in corrosion reactions.

RESULTS AND DISCUSSION

3.1 Surface morphology and elemental analysis

The SEM micrographs of the HA-316L SS-3, HA-316L SS-4 and HA-316L SS-5 coatings (Figure 1) revealed the development of smooth, high-coverage, uniform coatings. The HA-316L SS-3 and HA-316L SS-4 coatings were crack free but HA-316L SS-5 showed development of micro cracks. It has been reported that multiple dip coating lead to coatings more vulnerable to microcracking due to the combined effect of densification originated stresses and thermal stresses upon cooling after calcination. In accordance with EDX patterns, the intense peaks of Ca and P suggested the formation of HA coating over 316L SS substrate. However, in addition to Ca and P peaks in EDX patterns, peaks of Fe, Cr and Ni were also observed. The strength of these peaks increased in order given as: HA-316L SS-4 < HA-316L SS-5 < HA-316L SS-3. This suggested that HA coating had best coverage in HA-316L SS-4. Porosity in HA-316L SS-3, HA-316L SS-4 and HA-316L SS-5 were 0.91%, 0.97% and 0.79% respectively.

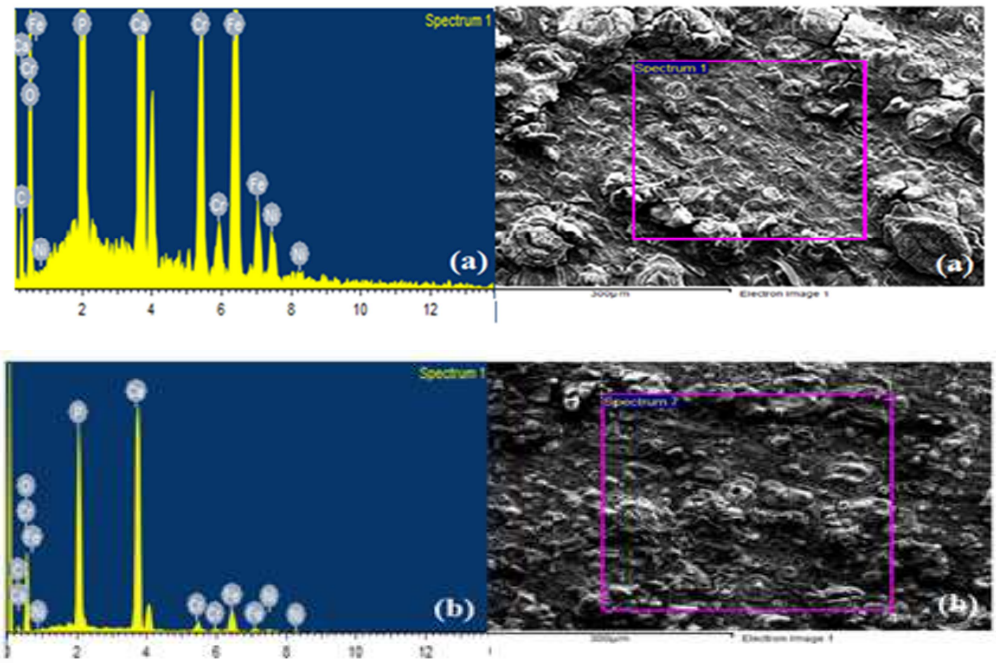

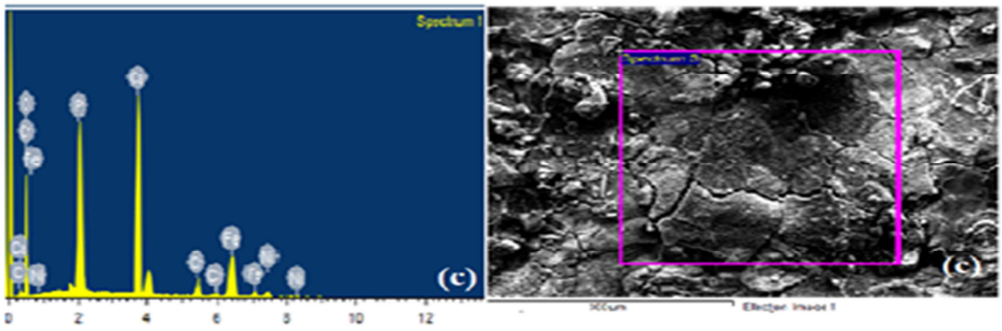

Figure1: SEM and EDX pattern of a) HA-316L SS-3, b) HA-316L SS-4, c) HA-316L SS-5 coatings

3.2 Mechanical properties

The average surface roughness (Ra), vicker's micro hardness and adhesion strength of HA-316L SS-3, HA-316L SS-4 and HA-316L SS-5 coatings are given in Table 2.

Table 2: Average surface roughness (Ra), vicker's micro hardness and adhesion strength of HA-316L SS-3, HA-316L SS-4 and HA-316L SS-5 coatings

Coating	Ra (µm)	Vicker's Micro Hardness (HV_{25})	Adhesion Strength (MPa)
HA-316LSS-3	0.123 ± 0.2	91.55	30.52
HA-316LSS-4	0.103 ± 0.2	138.8	46.27
HA-316LSS-5	0.204± 0.2	80.5	26.83

3.3 Linear potentiodynamic polarization

Figure 2 presents the linear potentiodynamic polarization curves uncoated 316L SS, HA-316L SS-3, HA-316L SS-4 and HA-316L SS-5. The polarization curves of coatings were shifted towards the higher potentials and lower current densities with respect to uncoated 316L SS which clearly indicated an improvement in corrosion resistance on coating of 316L SS with HA. The electrochemical parameters obtained from polarization measurements such as corrosion current density (I_{corr}), corrosion potential (E_{corr}), cathodic and anodic Tafel slopes (b_a, b_c) and rate of corrosion (mm/year) are given in Table 3.

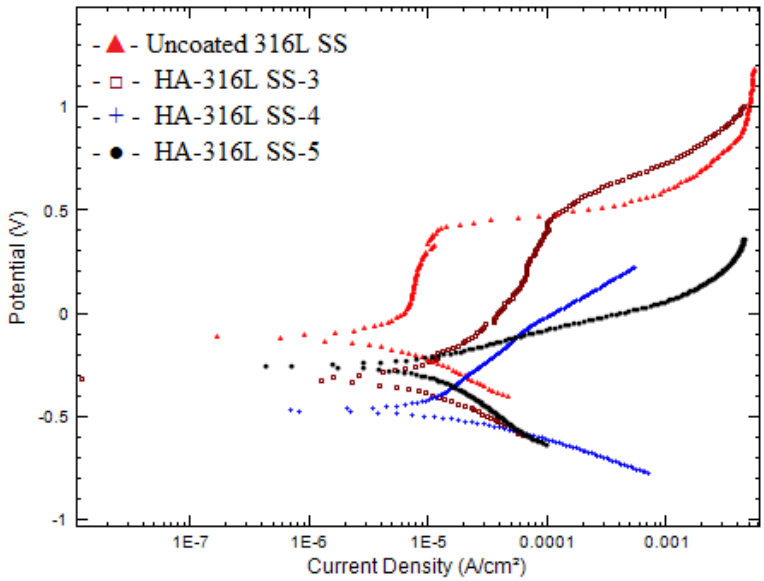

Figure 2: Potentiodynamic linear polarization curves for uncoated 316L SS, HA-316L SS-3, HA-316L SS-4 and HA-316L SS-5 in SBF solution at 37° C

Table 3: Corrosion parameters from potentiodynamic polarization tests for uncoated 316L SS, HA-316L SS-3, HA-316L SS-4 and HA-316L SS-5 in SBF solution at 37° C

Sample	OCP (V)	ba (mV/decade)	bc (mV/decade)	Ecorr (V)	Icorr (μA/cm²)	Corrosion rate(mm/year)
Uncoated 316LSS	-0.006	209.95	894.54	-148.63	4.29	0.049
HA-316LSS-3	-0.191	166.72	108.16	-303.79	2.80	0.032
HA-316LSS-4	-0.156	25.54	24.27	-470.42	1.09	0.012
HA-316LSS-5	-0.131	83.97	62.75	-249.83	2.45	0.028

The uncoated 316L SS, HA-316L SS-3, HA-316L SS-4 and HA-316L SS-5 arranged in an increasing order according to their OCP values are: uncoated 316L SS < HA-316L SS-3 < HA-316L SS-4 < HA-316L SS-5. Uncoated 316L SS displayed the most negative OCP value of -0.156V (vs. Ag-AgCl) because of possible dissolution of metal ion on its surface. Higher OCP values for HA-316L SS-3, HA-316L SS-4 and HA-316L SS-5 demonstrated that HA coatings were successfully providing a protective layer over 316L SS surface, thus preventing the occurrence of corrosion. Particularly, HA-316L SS-4 coating showed more satisfactory protection upon 316L SS than HA-316L SS-3 and HA-316L SS-5.The current density (I_{corr}) is commonly used to evaluate the corrosion rate. The corrosion rate is normally proportional to the current density measused through polarization studies. The potentiodynamic linear polarization curves suggested the corrosion protection of 316L SS by HA coatings, in terms of corrosion potential and current density and corrosion rate, increases in the order: HA-316L SS-4 < HA-316L SS-5 < HA-316L SS-3. Generally, sol-gel coated samples corrode through physical defects (holes) in the coating, allowing electrolyte access to the metal surface [28]. Essentially, particulate sol-gel derived coatings contain very fine porosities, since they are prepared at low temperature. Therefore, the inferior corrosion resistance of the HA-316L SS-3 and HA-316L SS-5 is due to the highly porous nature of former and presence of cracks in the later, which perhaps allowed electrolyte access to the substrate surface. Nevertheless, it was found that the HA-316L SS-4 exhibited better corrosion protection than HA-316L SS-3 and HA-316L SS-5 perhaps due to better adhesion to substrate and lower level of defect, which blocked the electrochemical process that otherwise would have occurred at the metal substrate surface.

CONCLUSION

In this work, hydroxyapatite coatings have been successfully deposited on 316L SS using sol–gel dip coating technique. The three coatings were developed by subjecting the substrate to three, four and five number of dips in the sol. All coatings showed high-coverage and good uniformity but HA-316L SS-5coating showed development of micro cracks. Porosity in HA-316L SS-3, HA-316L SS-4 and HA-316L SS-5 was 0.91%, 0.97% and 0.79% respectively. Among the HA-316L SS-3, HA-316L SS-4 and HA-316L SS-5 coatings, the HA-316L SS-4 demonstrated the minimum surface roughness, maximum micro hardness and adhesion strength. According to potentiodynamic polarization experiments, the HA-316L SS-4 coating offered a better corrosion protection of 316L SS substrate, compared to HA-316L SS-3 and HA-316L SS-5 coatings, because it provided better adhesion to substrate and porosity was not connected to substrate surface which blocked the electrochemical process that otherwise would have occurred at the metal substrate surface.

REFERENCES

[1] Balamurugan, S. Kannan, S. Rajeswari, *Materials Letters* 59 (**2005**) 3138-3143.
[2] C. Garcia, S. Cere, A. Duran, *Journal of Non-Crystalline Solids* 348 (**2004**) 218-224.
[3] L. Guo, H. Li. *surface & Coatings Technology* 185 (**2004**) 268-274.
[4] J. Harle, H.W. Kim, N. Mordan, J.C. Knowles, V. Salih, *ActaBiomaterialia* 2 (**2006**) 547-556.
[5] K. Chenga, S. Zhanga, W. Weng, X. Zeng, *Surface & Coatings Technology* 198 (**2005**) 242-246.
[6] V. Deram, C. Minichiello, R.N. Vannier, A. Le Maguer, L. Pawlowski, D. Murano, *J Surface and Coatings Technology*, 166 (2/3) (**2003**) 153-159.
[7] M. MazarAtabaki, J. Rabi'atuladawiyah, J. Idris, *Metalurgija*, 6(3) (**2010**) 49-163.
[8] P.A. Ramires, A. Romito, F. Cosentino, E. Milella, *Biomaterials* 22 (**2001**)1467-1474.
[9] K. De Groot, R.G.T. Geesink, C.P.A.T. Klein, P. Serekion, *J. Biomed Mater Res*., 21 (**1987**) 1375-81.
[10] A.E. Porter, L.W. Hobbs, R.V. Benzra, *Biomaterials*, 23 (3) (**2002**) 725-733.
[11] Y.P. Lu, M.S. Li, Z.G. Wang, *Biomaterials*, 25 (18) (**2004**) 439-440.
[12] S.J. Ding, C.P. Ju, L.J.H. Chern, *J. Bio-medicine Mater. Res*., 44 (3) (**1999**) 266-279.

[13] J.E.G. Hulshof, K. van Dijk, J.P.C.M. van der Waerden , J.G.C. Wolke, L.A. Ginsel , J.A. Jansen, *J. Biomed Mater. Res*., 29 (**1995**) 967-975.
[14] M. Wei, AJ. Ruys, B.K. Milthorpe, C.C. Sorrell, *J Biomed Mater. Res*., 45 (**1999**) 11-19.
[15] P. Ducheyne, W. Van Raemdonck, J.C. Heughebaert, M. Heughebaert, *Biomaterials*, 11 (**1990**) 244.
[16] Z. Xuhui, Y. Lingfang, Z. Yu, X. Jinping, *Chinese Journal of Chemical Engineering*, 17 (3) (**2009**) 667-671.
[17] C.T. Kwok , P.K. Wong , F.T. Cheng , H.C. Man, *Applied Surface Science* 255 (**2009**) 6736-6744.
[18] W. Xu, W. Hu, M Li, C. Wen, *Materials Letters*, 60 (**2006**) 1575-1578.
[19] D. Wang, G.P. Bierwagen, *Progress in Organic Coatings*, 64 (**2009**) 327-338.
[20] H.W. Kim, Y.M. Kong, C.J. Bae, Y.J. Noh, H.E. Kim, *Biomaterials*, 25 (**2004**) 2919- 2926.
[21] M.F. Hsieh, L.H. Perng, T.S. Chin, *Materials Chemistry and Physics*, 74 (**2002**) 245-250.
[22] D.M. Liu, T. Troczynski, W.J. Tseng, *Biomaterials*, 22 (**2001**) 1721-1730.
[23] T. Kokubo, T. Ito, S. Huang, Z.T. Hayashi, T. Sakka, T. Kitsugi, and T. Yamamuro, *Journal of Biomedical Materials Research*, (**1999**), 24, 331-343. doi:10.1002/jbm.820240306.
[24] T. Kokubo, H. Kushitani, S. Sakka, T. Kitsugi, and T. Yamamuro , *Journal of Biomedical Materials Research*, (**1990**), 24, 721- 734. doi:10.1002/jbm.820240607.
[25] A. Oyane, H.M. Kim, T. Furuya, T. Kokubo, T. Miyazaki, T. Nakamura, *Journal of Biomedical Materials Research*, 65, (**2003**), 188–195.
[26] M. Stern, A. Geary, Electochemical Polarization I. *J. Electrochem Soc*., 104 (**1957**) 56-63.
[27] G.M. Spinks, A.J. Dominis, G.G. Wallace, D.E. Tallman, *J. Solid State Electrochem*. 6 (**2002**) 85- 100.
[28] E. Setare, K. Raeissi, M.A. Golozar, M.H. Fathi, *Corrosion Science*, 51 (**2009**) 1802-1808.